The Astrophysical Journal, 618:919–925, 2005 January 10

MAGNETICALLY DRIVEN WINDS FROM POST–ASYMPTOTIC GIANT BRANCH STARS: SOLUTIONS FOR HIGH-SPEED WINDS AND EXTREME COLLIMATION

Guillermo García-Segura,[1] José Alberto López,[1] and José Franco[2]
Received 2004 June 7; accepted 2004 September 23

ABSTRACT

This paper explores the effects of post–asymptotic giant branch (AGB) winds driven solely by magnetic pressure from the stellar surface. It is found that winds can reach high speeds under this assumption and lead to the formation of highly collimated proto–planetary nebulae. Bipolar knotty jets with periodic features and constant velocity are well reproduced by the models. Several wind models with terminal velocities from a few tens of km s^{-1} up to 10^3 km s^{-1} are calculated, yielding outflows with linear momenta in the range 10^{36}–10^{40} g cm s^{-1}, and kinetic energies in the range 10^{42}–10^{47} ergs. These results are in accord with recent observations of proto–planetary nebulae that have pointed out serious energy and momentum deficits if radiation pressure is considered as the only driver for these outflows. Our models strengthen the notion that the large mass loss rates of post-AGB stars, together with the short transition times from the late AGB to the planetary nebula stage, could be directly linked with the generation of strong magnetic fields during this transition stage.

Subject headings: hydrodynamics — ISM: individual (He 2-90, He 3-401, M2-9, Mz 3, OH 231.8+4.2) — planetary nebulae: general — stars: AGB and post-AGB

1. INTRODUCTION

Winds from asymptotic giant branch (AGB) stars are thought to be driven by radiation pressure on dust grains (see review by Habing 1996), although an alternative physical mechanism has been proposed by Pascoli (1997) based on magnetic pressure transported out from the stellar interior to the stellar surface. On the other hand, it is widely accepted that planetary nebulae (PNs) are powered by line-driven winds emerging from their central stars and that they are formed from a two-wind dynamic interaction (i.e., Kwok et al. 1978). Evidence for this scenario is the large number of P Cygni line profiles detected in the central objects of planetary nebulae (Perinotto 1983).

Post-AGB stars with their associated proto–planetary nebulae (PPNs) are short-lived transition objects between AGB stars and white dwarfs. Their energy source, although unclear, has usually been assumed to be radiation pressure. However, recent observations of PPNs (Alcolea et al. 2001; Bujarrabal et al. 2001 and references therein) have revealed that the linear momenta and kinetic energies associated with these objects are in excess of what can be provided by radiation pressure alone, in some cases by up to 3 orders of magnitude. These large amounts of momentum and energy, as discussed in detail by Bujarrabal et al. (2001), cannot be accounted for by radiation pressure on dust grains, line-driven winds, or continuum-driven winds.

The results discussed by Pascoli (1997), based on surface magnetic pressure as the main driver of the large mass loss rates in AGB stars, are an attractive alternative to generate the required mechanical power in the winds of post-AGB stars, provided that the generation of magnetic fields can be efficient in post-AGB stars, as suggested by Blackman et al. (2001). Important indications that this may actually be happening in some objects are found in the OH maser radio observations of the PPN K3-35 by Miranda et al. (2001), revealing the existence of milligauss-strength fields in a magnetized torus around the PPN. Also, radio observations of PPNs CRL 2688 and NGC 7027 by Greaves (2002) show evidence of the presence of toroidal magnetic fields. A closely related result is that some nebulae, such as Menzel 3 (Santander-García et al. 2004), show an increasing degree of collimation with time, indicating that the internal B field may get stronger as the evolution proceeds. These observational data indicate that magnetically driven outflows, such as those discussed by Pascoli, could be a plausible mechanism to power the winds from post-AGB stars. In this case, in order to make a quick transition from the late-AGB to the post-AGB stages, the stellar wind should cause a steep increase in the magnetic field strength that would allow the star to blow away a good fraction of its remaining envelope.

There is not yet a clear model of how a single star can achieve this. One plausible scheme is that the rotation rate and the field strength at the stellar core increase during the formation of the white dwarf. Thus, the inner magnetic field becomes stronger as the core contracts and becomes exposed at the stellar surface when the envelope is peeled off during the PN formation. Thus, a strong and dominant toroidal component develops at the interface between the core and the envelope, where some dynamo action is expected, which may be responsible for launching a magnetically driven wind. Actually, Blackman et al. (2001) and Matt et al. (2004) have proposed that the post-AGB wind is produced by magnetocentrifugal processes when dynamo activity increases the internal field (see Blackman 2004) and the AGB star sheds its outer layers, exposing the rotating and magnetized core. Obviously, more detailed stellar interior studies with rotation and B fields are needed to understand the details of this issue. In addition, some authors have suggested that this may also occur in binary systems and, for instance, Soker (1997) proposed that the post-AGB stellar core can be spun up by a secondary, increasing the shear between the core and the envelope. Similarly, the spiral-in process of a secondary star or a giant planet may also be able to produce a large shear in the stellar envelope and raise the magnetic field strength by dynamo activity (Tout & Regös 2003). These cases link the

[1] Instituto de Astronomía-UNAM, Apdo Postal 877, Ensenada 22800, Baja California, Mexico; ggs@astrosen.unam.mx, jal@astrosen.unam.mx.
[2] Instituto de Astronomía-UNAM, Apdo Postal 70-264, México 04510, México D. F., Mexico; pepe@astroscu.unam.mx.

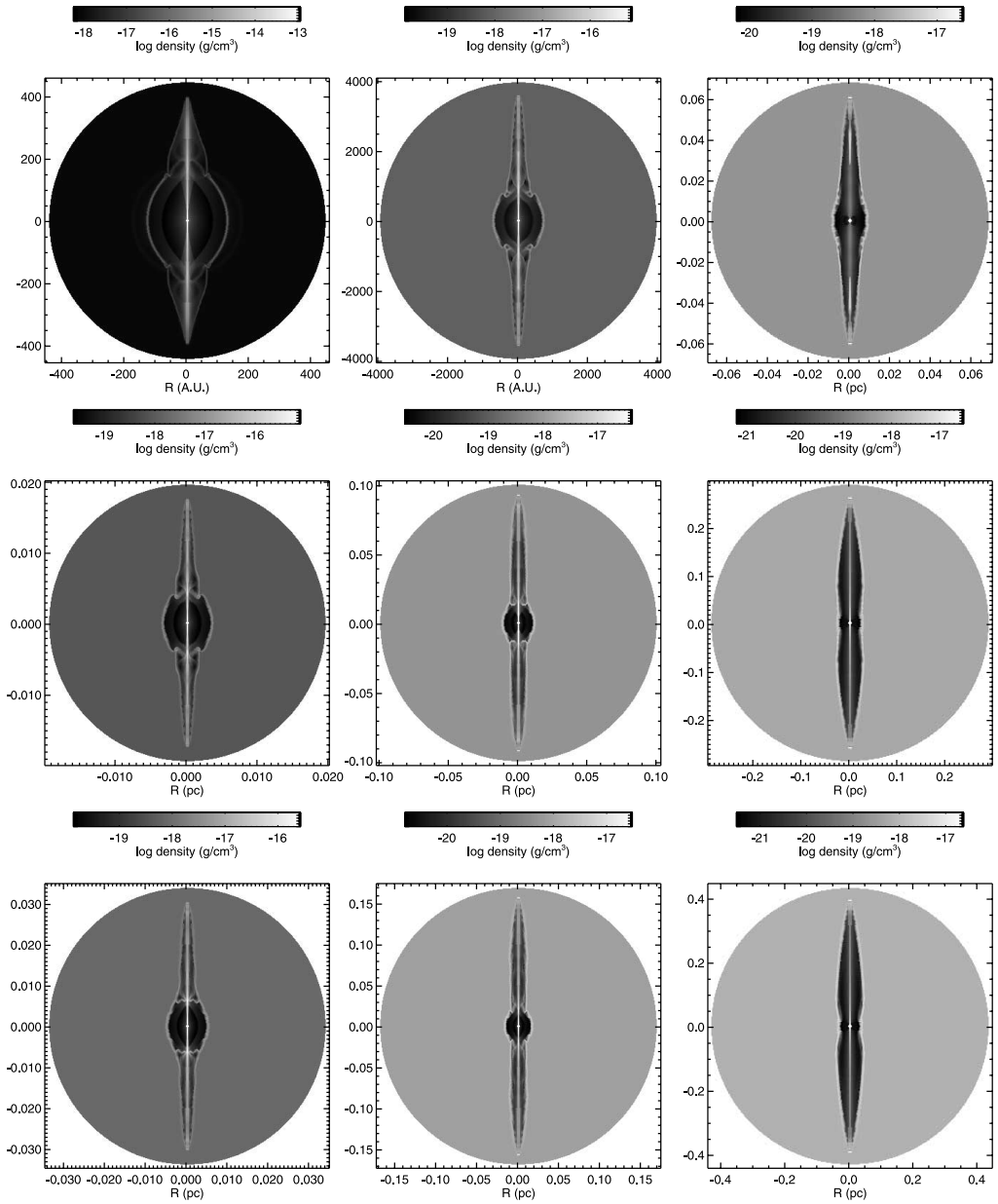

FIG. 1.—Logarithm of density for models A (0.1 G, *left*), B (1 G, *middle*), and C (5 G, *right*) at three different epochs, 50 yr (*top*), 500 yr (*middle*), and 1000 yr (*bottom*). Note the change in the spatial scale.

large mass loss rates in the post-AGB stages with a common-envelope phase. Unfortunately, there are very few detailed studies of post–common-envelope systems (e.g., Exter et al. 2003). Here we do not select any particular scenario for creating a strong toroidal stellar field, and focus our study only in what occurs after a strong magnetized wind is created.

In previous papers (Różyczka & Franco 1996; García-Segura 1997; García-Segura et al. 1999; García-Segura & López 2000), we have assumed magnetized, line-driven winds in the range 10^2–10^3 km s^{-1}, with radial magnetic fields at the stellar surface. As in the case of the solar wind, the magnetic fields are primarily poloidal and parallel to the flow at small distances from the star, stellar rotation creates a toroidal component, and the hoop stress only plays an important role at large distances from the star. These solutions seem appropriate to model PNs with hot central stars, in which line-driven winds should be operative. In this paper we simply consider that the surface magnetic fields are increased during the transition toward the post-AGB stage and investigate the effects of mass loss when this is dominated by magnetic pressure, as suggested by Pascoli (1997). Here the wind is computed from the stellar surface and is solved from sonic velocity up to the terminal velocity. For simplicity, the toroidal magnetic field at the stellar surface is the main and only driver of the wind. This is an idealized, simple case, but it allows us to study the effects of a magnetically driven wind. Section 2 describes the numerical procedure, § 3 presents and discusses the numerical results, and § 4 presents the conclusions.

2. NUMERICAL MODELS

A novel aspect in this paper is that the stellar wind is not imposed at the inner boundary; instead, it is computed with a simple scheme. We set an initial cold (100 K), isothermal atmosphere with a power-law density stratification $\rho \sim r^{-2}$, corresponding to a spherically symmetric wind with $\dot{M} = 1 \times 10^{-6}\ M_\odot\ \mathrm{yr}^{-1}$ and $v_\infty = 10$ km s^{-1}. These are just reference values in order to compute the density. The stellar gravitational

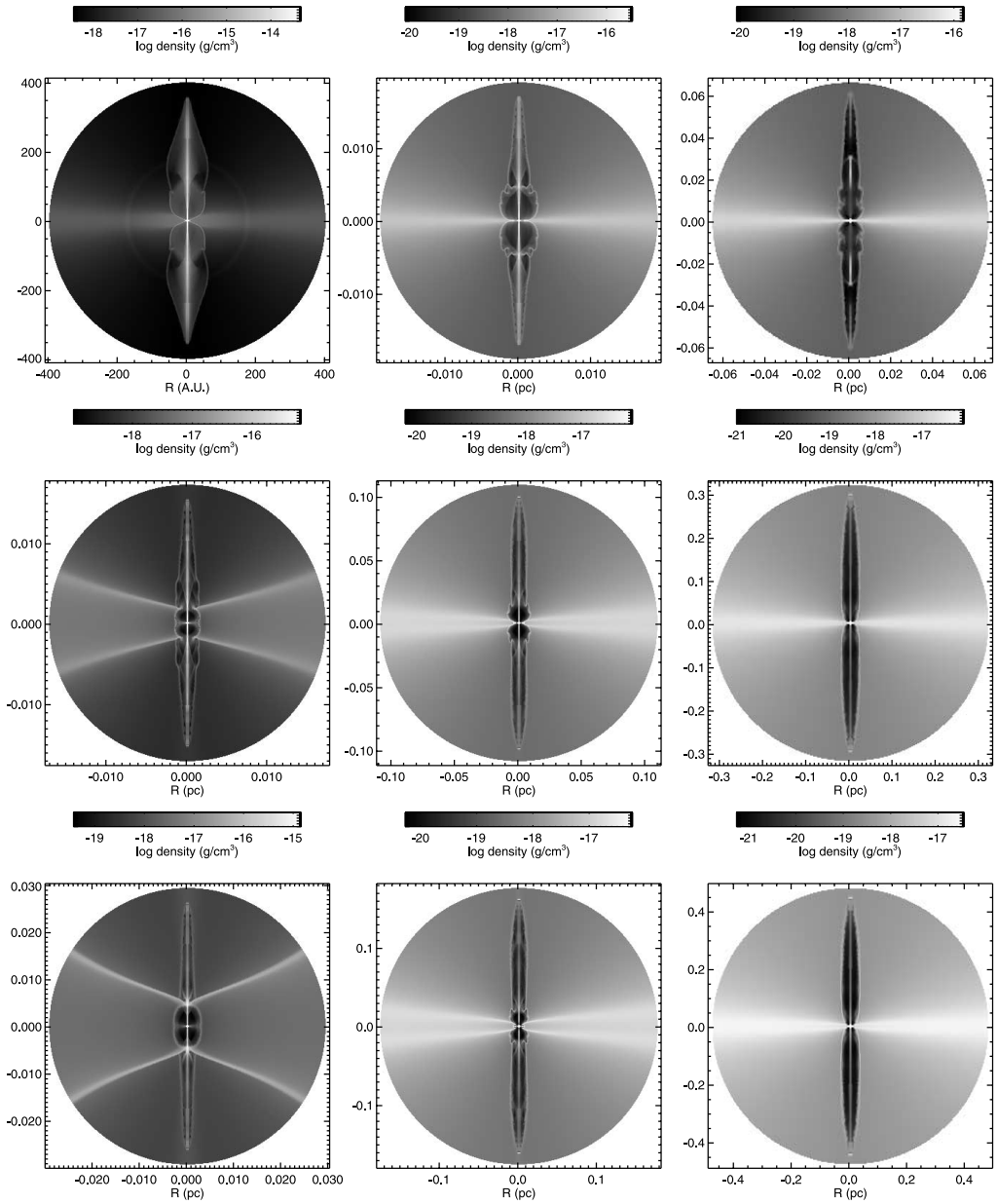

FIG. 2.—Logarithm of density for models D (0.1 G, *left*), E (1 G, *middle*), and F (5 G, *right*) at three different epochs, 50 yr (*top*), 500 yr (*middle*), and 1000 yr (*bottom*). Note the change in the spatial scale. These models include a equatorial density enhancement.

field is always included as an external force that corresponds to a point mass of 1 $M_\odot$. We set outward sonic velocity to the wind and to the stellar surface (i.e., the initial conditions are almost static and, without any additional force, the whole atmosphere would collapse in a free-fall timescale). Once the grid is filled up with these conditions, a toroidal magnetic field is introduced at the stellar surface with a latitude dependence of the form

$$B_\phi(\theta) = B_s \sin\theta, \tag{1}$$

where B_s is the field at the equator ($\theta = \pi/2$). In contrast to our previous papers, in which the surface magnetic field corresponds to the radial component of the field, here we follow Pascoli (1997) and B_s is a pure toroidal component. It is precisely the magnetic pressure at the stellar surface ($\sim B_s^2$) that makes the atmosphere expand, resulting in a magnetically driven stellar wind. Since radiation pressure is not included here, the present model illustrates the impact and importance of magnetic effects. A more realistic model, combining both radiation and magnetic pressures and the contribution of a poloidal component of the field, will be the subject of a future work.

To compute the time evolution of the initial conditions described above, we have performed the simulations using the magnetohydrodynamic code ZEUS-3D (ver. 3.4), developed by M. L. Norman and the Laboratory for Computational Astrophysics. This is a finite-difference, fully explicit, Eulerian code descended from the code described in Stone & Norman (1992). A method of characteristics is used to compute magnetic fields, as described in Clarke (1996), and flux freezing is assumed in all the runs. We have used spherical polar coordinates (r, θ, Φ), with reflecting boundary conditions at the equator and polar axis. Rotational symmetry is assumed with respect to the polar axis, and our models are effectively two-dimensional. The simulations are carried out in the meridional (r, θ) plane, but three

independent components of the velocity and magnetic field are computed (i.e., the simulations are in 2.5 dimensions).

3. RESULTS AND DISCUSSION

3.1. *Post-AGB Wind Models*

We have first verified our method by using as input stellar conditions the same parameters used by Pascoli (1997) for an AGB star, namely, $M = 1.1\ M_\odot$, $R_s = 2$ AU, $B_s = 40$ G, and $\rho_s = 3.5 \times 10^{-10}$ g cm^{-3}.

Our grid consists of 200×180 equidistant zones in r and θ, respectively. The innermost radial zone lies at $r_i = 2$ AU, just at the stellar surface, and the outermost zone is at $r_o = 80$ AU. The angular extent is 90°. For these values, we obtain for the asymptotic velocity $v_\infty = 17.7$ km s^{-1} at $r = 40R_s$ (i.e., 80 AU), in the range 10–20 km s^{-1}, in close agreement with the values obtained by Pascoli (1997). Our solution also agrees in shape with his Figure 3 (case $1/x^2$).

The next step is to select a stellar candidate to compute solutions for post-AGB winds. We have selected from the literature the well-studied object OH 231.8+4.2 (Sánchez-Contreras et al. 1997; Alcolea et al. 2001; Bujarrabal et al. 2002; Jura et al. 2002; Desmurs et al. 2002), which has a cool (M9 III, $T \sim 2000$ K) central star with $M \approx 1\ M_\odot$, $R_s = 4.5$ AU, and a rotation velocity of $v_{\rm rot} = 6$ km s^{-1}. This object is a member of the open cluster NGC 2437 (M46), with an estimated initial mass of $M_{\rm ZAMS} = 3\ M_\odot$.

We have computed three wind solutions, S1, S2, and S3, with surface magnetic fields of 0.1, 1, and 5 G, respectively. The asymptotic terminal velocity has been measured at $r = 40R_s$, just above the equatorial plane, obtaining the values 34, 374, and 1874 km s^{-1}, respectively. These solutions are computed with a fixed grid in which the innermost radial zone lies at $r_i = 4.5$ AU, just at the stellar surface, and the outermost zone at $r_o = 180$ AU. The computations stop when the solutions become steady state. These results show the ability of toroidal fields to drive stellar winds in the range of a few tens of km s^{-1} up to 10^3 km s^{-1}.

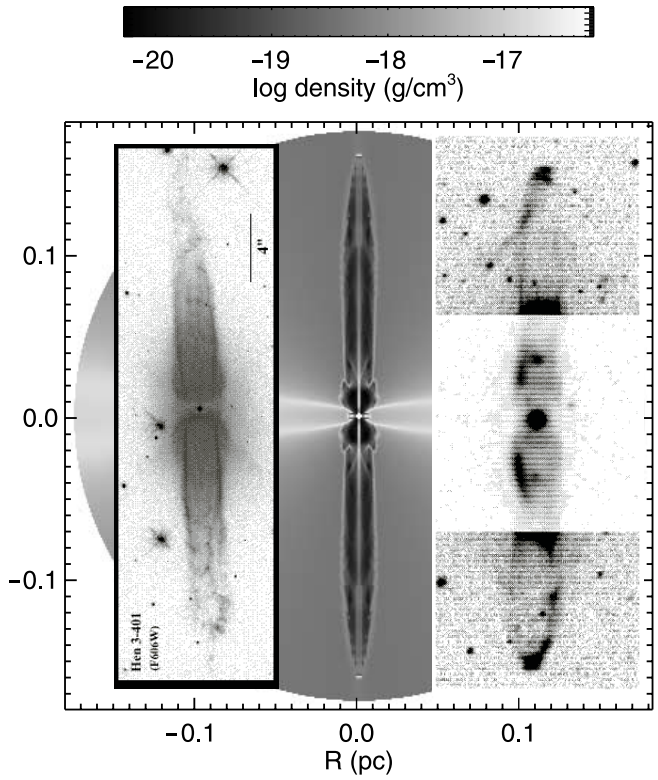

FIG. 3.—Logarithm of density for model E (1 G) at 1000 yr of its evolution (*middle*) compared to He 3-401 (Sahai 2002; *left*) and M2-9 (Schwarz et al. 1997; *right*).

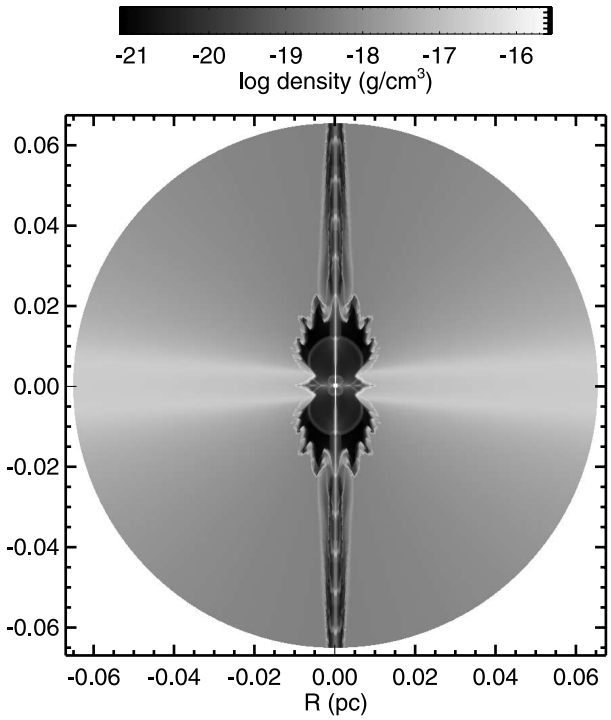

FIG. 4.—Logarithm of density for model G, a similar model to E but with a magnetic cycle of 80 yr. Every 40 yr a pair of blobs are formed at the polar axis.

3.2. *Proto–Planetary Nebula Models*

As a next step, we study the type of nebulae that magnetized post-AGB wind models are able to generate.

A self-expanding grid technique similar to that used by Jun & Norman (1996) has been used in order to allow the spatial coordinates to grow by several orders of magnitude. Our expanding grids consist of 200×180 equidistant zones in r and θ, respectively. The initial innermost and outermost radial zones are as described before. These values are used only up to the point at which a shock approaches the outermost boundary. After that, a shock-tracking routine evaluates the expansion velocity for each forward shock (v_s) at the polar axis and produces a self-expanding grid as $v_g(i) = v_s[r(i)/r_s]$, where $v_g(i)$ and $r(i)$ are the velocity and position of each grid zone in the r-coordinate and r_s is the position of the shock wave. Thus, the final grid size depends on the dynamical evolution of each individual run. The angular extent is 90° in all cases.

Using this expanding-grid technique, we have followed the wind expansion and nebula formation for six models using the same inputs as before (S1, S2, and S3). Three of them, models A, B, and C, have a spherically symmetric initial atmosphere (Fig. 1), while models D, E, and F (Fig. 2) have an equatorial density enhancement. To produce this enhancement, we have used the same scheme described in García-Segura et al. (1999), based on the wind compressed zone solutions of Bjorkman & Cassinelli (1993), adopting a stellar rotation velocity of 6 km s^{-1} as observed in OH 231.8+4.2. The outer radial boundary

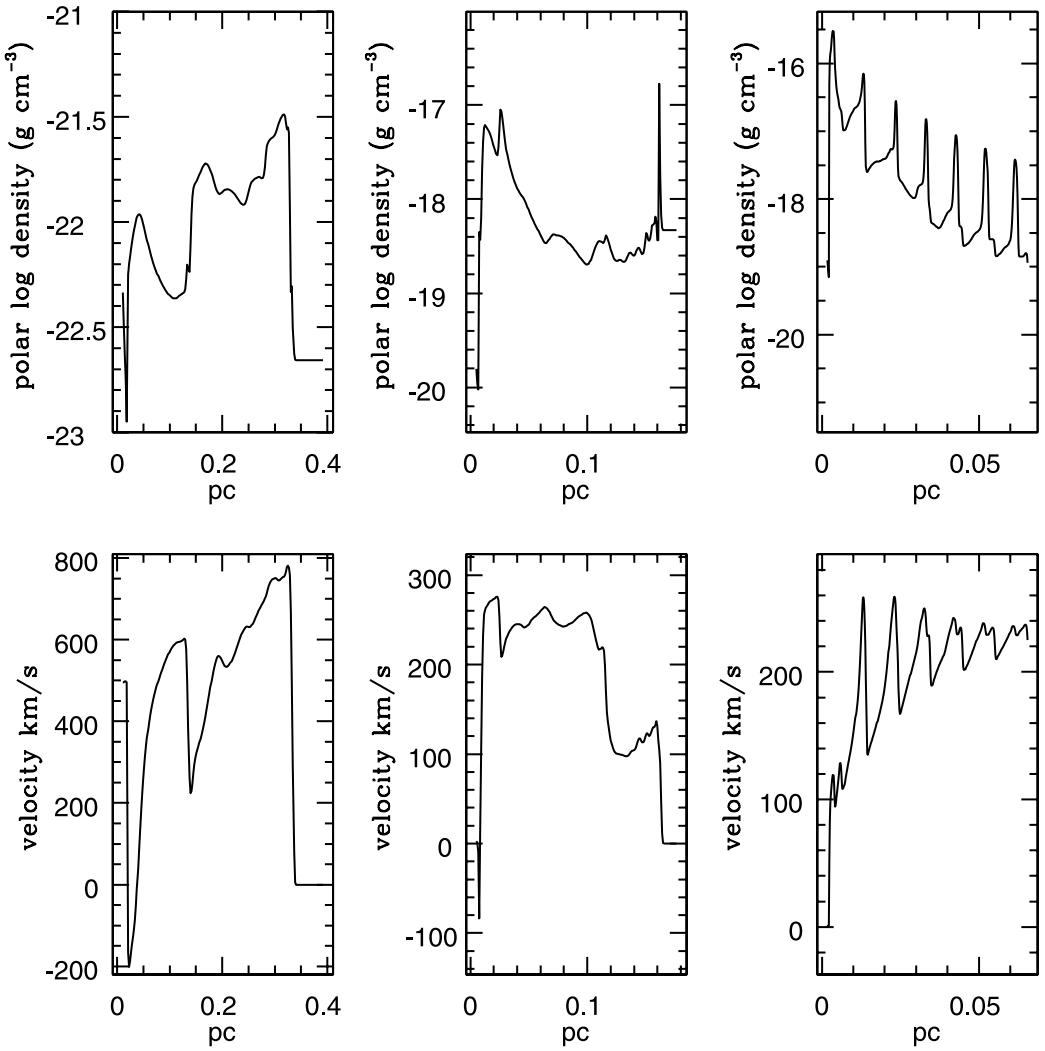

FIG. 5.—Logarithm of density (*top*) and polar velocity (*bottom*) of three different cases. On the left, an example of a magnetized line-driven wind with $\sigma = 0.1$ (model U in García-Segura et al. 1999). Middle panels correspond to model E, a magnetically driven wind. Right panels correspond to model G, a periodic, magnetically driven wind.

is updated properly at each loop, following the expansion of the grid.

The numerical solutions show that collimation is well established at the very early phases of evolution, creating jet-like outflows at locations close to the star. The inclusion of the density enhancement (Fig. 2) produces, as expected, a narrow equatorial waist without any apparent direct impact at the polar regions. The polar expansion velocities are similar for all models with the same input magnetic field; models A and D have $v_{\rm exp} \sim 30$ km s^{-1}, models B and E have $v_{\rm exp} \sim 150$ km s^{-1}, while models C and F have $v_{\rm exp} \sim 390$ km s^{-1}.

As a comparative example, Figure 3 compares the result of one of the models with 1 G (model E) at 1000 yr with two well-known, extremely collimated PPNs, He 3-401 (Sahai 2002) and M2-9 (Schwarz et al. 1997). It is apparent in this figure that the solution is able to convincingly reproduce the extreme collimated shapes, along with the sizes and kinematics of these nebulae.

3.3. *Magnetic Cycles*

Magnetic cycles, and their associated field reversals, have been proposed as a plausible origin for the existence of multiple, regularly spaced, and faint concentric shells around some planetary nebulae observed with the *Hubble Space Telescope* (Soker 2000; García-Segura et al. 2001). In fact, OH maser observations by Szymczak et al. (2001) suggest that changes in the polarized maser emission in some stars could be caused by turbulence in the circumstellar magnetic field and by global magnetic field reversals. Here then we also explore the effects of magnetic field reversals in magnetically driven winds, and compare the results with objects displaying collimated outflows with periodic outburst features. An interesting example is He 2-90, a PPN whose symmetric and highly collimated, knotty, bipolar outflow was described by Sahai & Nyman (2000). The radial velocities of the knots have been measured by Guerrero et al. (2001), and the corresponding proper motions have subsequently been derived by Sahai et al. (2002). An interesting and puzzling characteristic in this case is that the collimated outflow, or jet, maintains a nearly constant apparent width throughout all its extent, i.e., it does not fan out at large distances from the star, and the velocity of the regularly spaced knots seems to be the same. The "jet" speed is somewhere between 150 and 360 km s^{-1}, its dynamical time is at least 1400 yr, and the knots are created at the rate of one pair roughly every 35–45 yr.

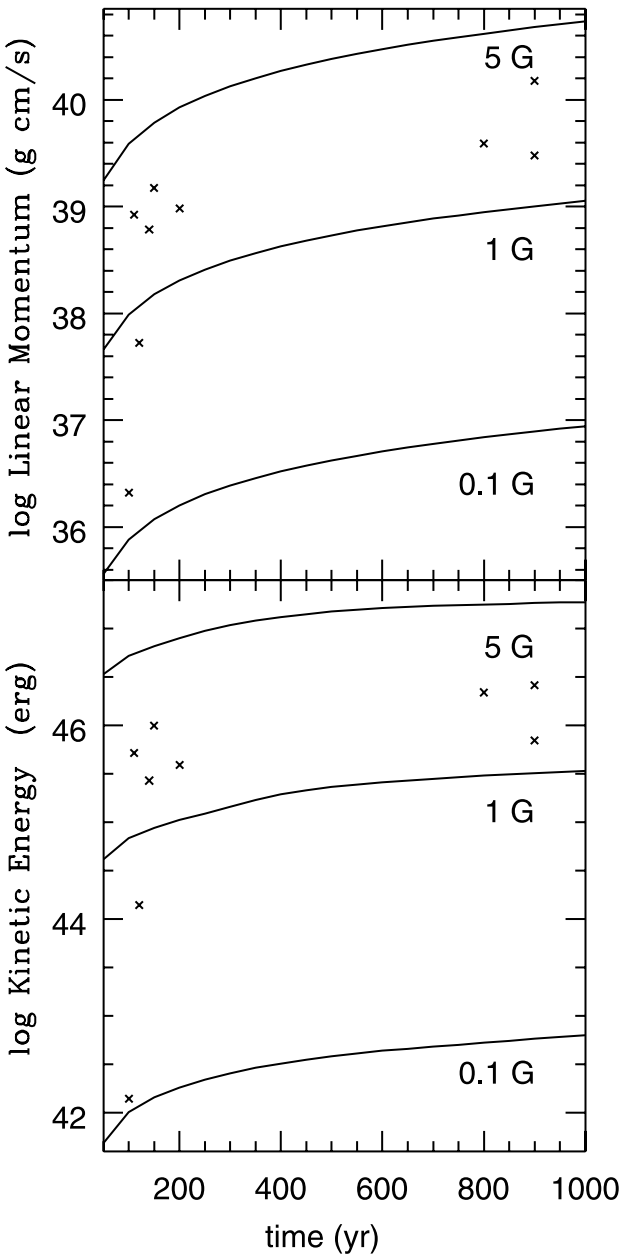

FIG. 6.—Evolution of total linear momentum (*top*) and total kinetic energy (*bottom*) gained by models A (0.1 G), B (1 G), and C (5 G). Available observations (*crosses*) are taking from Bujarrabal et al. (2001).

We have computed model G (similar to E, and shown in Fig. 4) with a simple treatment of the stellar magnetic field (B_s), allowing it to change sign in a cycle of the form

$$B_s(t) = B_{\max} \cos\left(2\pi \frac{t}{P}\right), \quad (2)$$

where $B_{\max}$ is the maximum equatorial B-field at the stellar surface and P is the period of the magnetic cycle. Since we do not know the true variation form of the field, this functional form is just a first-order, simple approximation, and is the same scheme used by García-Segura et al. (2001) to model the concentric rings around PNs and PPNs. As in the case of the Sun, we assume that $B_{\max}$ has opposite signs at each hemisphere, with a neutral current sheet near the equatorial plane (e.g., Wilcox & Ness 1965; Smith et al. 1978). The average thickness of the neutral current sheet in the solar case is $\sim 10^8$ cm, and its presence does not affect the field outside the equatorial sections. For simplicity, given that we compute only one hemisphere, we neglect the size of this current sheet. Values for P are adopted arbitrarily in order to match the only source of observational information available in this regard, namely, the estimated production of knots. We have used a period of 80 yr for the magnetic cycle to match the observational data. Thus, every 40 yr a new pair of blobs are produced.

The results of the simulations for model G are shown in Figure 4. It is apparent from this figure that the similarities of the model to He 2-90 are remarkable. The highly collimated outflow and its periodic knotty structure are both well reproduced, as is the global kinematics (see next section). Thus, in spite of the highly simplified model assumptions, the results indicate that magnetically driven winds are able to offer a reasonable explanation for the formation of highly collimated, knotty bipolar jets with the periodic characteristics in PPNs. Furthermore, the kinematics of the jets that originate from magnetically driven winds are different from that produced by magnetized, line-driven winds. While magnetized line-driven winds produce observable jets with linearly increasing velocity with distance, the so-called Hubble flows (Fig. 5; see also García-Segura et al. 1999), magnetically driven winds produce a much more constant pattern in velocity (Fig. 5). Thus, these differences in the kinematic behavior could be useful in distinguishing the type of mechanism involved in the launching process of the corresponding outflows.

3.4. *Mechanical Energy in the Outflows*

We now turn our attention to the kinetic energy and linear momentum contained in the outflows from these models. Bujarrabal et al. (2001), as mentioned earlier, have pointed out that radiation pressure is insufficient to provide the observed mechanical power in the outflows of PPNs. Figure 6 gives the results for three different values of the surface magnetic fields covering the initial 1000 yr of evolution. The data of PPNs from Bujarrabal et al. (2001) are indicated as crosses in these plots. The values for most of these objects seen to be well bracketed by models B (1 G) and C (5 G). Therefore, magnetically driven winds are able to provide the necessary energy budget to power the outflows of PPNs.

4. CONCLUSIONS

The origin and evolution of PPNs and PNs represent one of the key questions in our understanding of stellar physics. Modeling the fascinating features displayed by these objects requires not only a better knowledge of stellar structure at the AGB stage (and beyond) but also a proper consideration of the driving mechanisms for mass ejection. The transition from AGB to post-AGB to PN central stars involves drastically different conditions at every stage. Whereas radiation pressure on dust grains is the most likely mechanism at the AGB phase, as are line-driven winds in the case of PN central stars, for post-AGB stars the details of the driving force has been relatively unexplored. A promising avenue, using dynamo amplification at these late evolutionary stages, has been discussed by Matt et al. (2004). They use a simplified model in which the interface between the (rotating and magnetized) stellar core and envelope stores a large amount of magnetic energy because of the twisting of an originally poloidal magnetic field. The magnetic energy is extracted from the stellar rotational energy, causing a rapid spin-down of the proto–white dwarf, and is able to drive

a strong and short outburst (this is somewhat similar to the ''magnetic bubble'' mechanism proposed by Draine 1983 to generate molecular outflows in star-forming clouds). The outflow can expel the envelope and is termed ''magnetic explosion'' by Matt et al.

Indeed, here we do not explore a self-consistent mechanism to generate magnetic energy but show that a sudden increase of the magnetic field at the onset of the post-AGB stage can lead to prominent magnetically driven stellar winds. These winds are able to reproduce some of the important characteristics observed in these transition objects, such as high mass loss rates, short transition times from the late-AGB to the PN stage, extreme collimation of the developing nebular shell, and high outflow velocities. In addition, flat kinematic trends in the outflows and periodic features, as observed in some cases, can also be explained. Furthermore, the apparently puzzling energy deficit to power the outflows in this stage is solved if magnetic drivers are considered. Here we have concentrated on exploring the effects of winds driven by toroidal fields, but future studies will include the contribution of additional ingredients, such as radiation pressure and the poloidal magnetic component. Clearly, more work is required to understand the details of the growth of surface magnetic fields at the end of the AGB stage and their impact on the nebular structure and morphologies.

G. G.-S. thanks Noam Soker for fruitful discussions. As usual, we also thank Michael L. Norman and the Laboratory for Computational Astrophysics for the use of ZEUS-3D. The computations were performed at Instituto de Astronomía-UNAM. This work has been partially supported by grants from DGAPA-UNAM (IN130698, IN117799, and IN114199) and CONACyT (32214-E).

REFERENCES

Alcolea, J., Bujarrabal, V., Sánchez-Contreras, C., Neri, R., & Zweigle, J. 2001, A&A, 373, 932
Bjorkman, J. E., & Cassinelli, J. P. 1993, ApJ, 409, 429
Blackman, E. G. 2004, in ASP Conf. Ser. 313, Asymmetric Planetary Nebulae III, ed. M. Meixner et al. (San Francisco: ASP), 401
Blackman, E. G., Frank, A., Markiel, J. A., Thomas, J. H., & Van Horn, H. M. 2001, Nature, 409, 485
Bujarrabal, V., Alcolea, J., Sánchez-Contreras, C., & Sahai, R. 2002, A&A, 389, 271
Bujarrabal, V., Castro-Carrizo, A., Alcolea, J., & Sánchez-Contreras, C. 2001, A&A, 377, 868
Clarke, D. A. 1996, ApJ, 457, 291
Desmurs, J.-F., Sánchez-Contreras, C., Bujarrabal, V., Colomer, F., & Alcolea, J. 2002, in IAU Symp. 206, Cosmic Masers: from Protostars to Black Holes, ed. V. Migenes & M. J. Reid (San Francisco: ASP), 344
Draine, B. 1983, ApJ, 270, 519
Exter, K. M., Pollacco, D. L., & Bell, S. A. 2003, MNRAS, 341, 1349
García-Segura, G. 1997, ApJ, 489, L189
García-Segura, G., Langer, N., Różyczka, M., & Franco, J. 1999, ApJ, 517, 767
García-Segura, G., & López, J. A. 2000, ApJ, 544, 336
García-Segura, G., López, J. A., & Franco, J. 2001, ApJ, 560, 928
Greaves, J. S. 2002, A&A, 392, L1
Guerrero, M., Miranda, L. F., Chu, Y.-H., Rodríguez, M., & Williams, R. M., 2001, ApJ, 563, 883
Habing, H. J. 1996, A&A Rev., 7, 97
Jun, B.-I., & Norman, M. L. 1996, ApJ, 465, 800
Jura, M., Chen, C., & Plavchan, P. 2002, ApJ, 569, 964
Kwok, S., Purton, C. R., & Fitzgerald, P. M. 1978, ApJ, 219, L125
Matt, S., Frank, A., & Blackman, E. G. 2004, in ASP Conf. Ser. 313, Asymmetric Planetary Nebulae III, ed. M. Meixner et al. (San Francisco: ASP), 449
Miranda, L. F., Gómez, Y., Anglada, G., & Torrelles, J. M. 2001, Nature, 414, 284
Pascoli, G. 1997, ApJ, 489, 946
Perinotto, M. 1983, in IAU Symp. 103, Planetary Nebulae, ed. D. R. Flower (Dordrecht: Reidel), 323
Różyczka, M., & Franco, J. 1996, ApJ, 469, L127
Sahai, R. 2002, Rev. Mex. AA Ser. Conf., 13, 133
Sahai, R., Brillant, S., Livio, M., Grebel, E. K., Brandner, W., Tingay, S., & Lyman, L.-A. 2002, ApJ, 573, L123
Sahai, R., & Nyman, L.-A. 2000, ApJ, 538, L145
Sánchez-Contreras, C., Bujarrabal, V., & Alcolea, J. 1997, A&A, 327, 689
Santander-García, M., Corradi, R., Balick, B. & Manpaso, A. 2004, A&A, 426, 185
Schwarz, H. E., Aspin, C., Corradi, R. L. M., & Reipurth, B. 1997, A&A, 319, 267
Smith, E. J., Tsurutani, B. T., & Rosenberg, R. L. 1978, J. Geophys. Res., 83, 717
Soker, N. 1997, ApJS, 112, 487
———. 2000, ApJ, 540, 436
Stone, J. M., & Norman, M. L. 1992, ApJS, 80, 753
Szymczak, M., Blaszkiewicz, L., Etoka, S., & Le Squeren, A. M. 2001, A&A, 379, 884
Tout, C. A., & Regös, E. 2003, in ASP Conf. Ser. 293, 3D Stellar Evolution, ed. S. Turcotte, S. C. Keller, & R. M. Cavallo (San Francisco: ASP), 100
Wilcox, J., & Ness, N. 1965, J. Geophys. Res., 70, 1233